Bartosz Sułkowski

Effect of texture
on deformation mode in magnesium and AZ61 alloy

Wpływ tekstury
na mechanizmy deformacji magnezu i stopu AZ61

Abstract

The effect of the initial texture on the deformation mode and mechanical properties was studied in magnesium and its AZ61 alloy. Both materials had a very similar initial texture. Two cases were investigated: samples with a texture where the basal slip system was blocked, and samples having a texture where the basal slip system was allowed to activate. The samples were deformed by compression at room temperature at a strain rate of 10^{-3} s^{-1}. It was found that the initial texture had a very strong impact on the deformation mode in magnesium; however, there was no effect of the initial texture on the deformation mode in the case of AZ61. The investigations were compared to simulations of texture evolution using the Taylor model. From the simulations, the Taylor factor and slip system activity were obtained. It was found that, in the case of magnesium, twinning or slip (both basal and non-basal) are the two main deformation modes, while in the case of AZ61, slip is the only main deformation mechanism despite the initial texture. The impact of the initial texture is discussed in more detail in the present study.

Keywords: magnesium, AZ61, deformation, twinning, texture simulations, Taylor factor

Streszczenie

W pracy badano wpływ początkowej tekstury na mechanizmy deformacji i właściwości mechaniczne magnezu i stopu magnezu AZ61. Zbadano dwa przypadki: próbki, w których bazalny system poślizgu został zablokowany, oraz próbki, w których bazalny system poślizgu mógł być aktywowany. Próbki odkształcano przez ściskanie w temperaturze pokojowej z prędkością odkształcania 10^{-3} s^{-1}. Stwierdzono, że początkowa tekstura miała bardzo silny wpływ na sposób deformacji magnezu; jednak w przypadku AZ61 nie zauważono podobnego efektu wpływu początkowej tekstury na właściwości mechaniczne. Badania porównano z symulacjami ewolucji tekstury za pomocą modelu Taylora. Z symulacji uzyskano współczynnik Taylora i aktywności systemów poślizgu. Stwierdzono, że w przypadku magnezu, w zależności od początkowej tekstury, poślizg (zarówno w bazalnym systemie, jak i niebazalnych systemach poślizgu) oraz bliźniakowanie są dwoma głównymi mechanizmami deformacji, natomiast w przypadku AZ61 głównym mechanizmem deformacji, pomimo początkowej tekstury, jest tylko poślizg.

Słowa kluczowe: magnez, AZ61, deformacja, bliźniakowanie, modelowanie ewolucji tekstury, współczynnik Taylora

Bartosz Sułkowski: AGH University of Science and Technology, Faculty of Non-Ferrous Metals, Department of Non-Ferrous Metals Engineering, Krakow, Poland; sul5@agh.edu.pl

1. Introduction

Texture has a great impact on the mechanical properties of magnesium and its alloys. The texture effect is even more important in hexagonal metals because of the strong anisotropy of the HCP structure. The influence of the texture on the mechanical behaviors of magnesium and its alloys has been recently studied by various researchers [1–13]. It was shown by Gehrmann et al. [1] that, during the processing of the AZ31 magnesium alloy, higher work hardening and lower ductility exhibit samples that have an initial strong fiber texture (the c-axis along the compression direction) as compared to samples with the c-axis parallel to the sheet normal or rolling direction. Wang et al. [2] studied the effect of the initial texture on the characteristics of ZK60 subjected to the bending process. In the case of the samples prepared along the rolling direction, basal and prismatic slip were the two main deformation modes, while twinning in the (10$\bar{1}$2) system was the main deformation mode for the samples having a c-axis along the transverse direction. The effect of the different initial rolling textures on the formability of magnesium sheets was studied by Tadano [3] (based on simulations). It was found that the strong limit of the slip in the basal slip system was the result of the deviation of the c-axis from the compression direction. The AZ61 magnesium alloy during rolling and annealing was investigated by Sułkowski and Pałka [4]. It was found that the texture changed from a basal-type texture resulting from rolling to a texture that had a {10$\bar{1}$0} <11$\bar{2}$0> strong component after annealing. Processing samples with a basal-type texture resulted in failure, while samples with a {10$\bar{1}$0} <11$\bar{2}$0> texture component exhibited more ductility [4, 14].

In the present study, magnesium and its AZ61 alloy were investigated. Both materials had a similar starting texture. Moreover, two types of different starting textures were taken into account to involve different deformation modes. The first was a texture that had its c-axis along a radial direction, and the second type of texture had its c-axis along a normal direction – transverse direction. The texture was chosen in such a way as to inspect whether the initial texture is a decisive factor that has a strong influence on the deformation mode for the materials given.

2. Experiments

In the present study, magnesium with a purity of 99.8% and the AZ61 alloy with a chemical composition of Al 6%, Zn 1%, and Mg balanced were investigated. Both materials had a very similar initial texture (as shown in Figure 1). The two types of samples were prepared depending on the initial texture. The Type A samples (Figs. 1a, 1c, 1e, and 1g) had an extrusion-type texture, where the c-axis in the grains is along a radial direction. In this case, the basal slip should be blocked during compression and other deformation modes must be activated; e.g., non-basal slip systems or twinning. The Type B samples had a texture where the c-axis was along the path from a transverse direction (TD) to a normal

direction (ND) (see Figs. 1b, 1d, 1f, and 1h); in this case, the basal slip system should be the main deformation mode. Figures 1g and 1h show ideal {0002} pole figures calculated from the 10,000 grains generated using a special procedure described by Graff [15]. In the case of the pole figure shown in Figure 1e, the φ1 and φ2 Euler angles of each grain were taken at random within a range of −360° to 360°, while the Φ was random within a range of −10° to 10°. In the case of the pole figure shown in Figure 1h, the φ1 and Φ were within a range of −360° to 360°, and the φ2 was within a range of −10° to 10°.
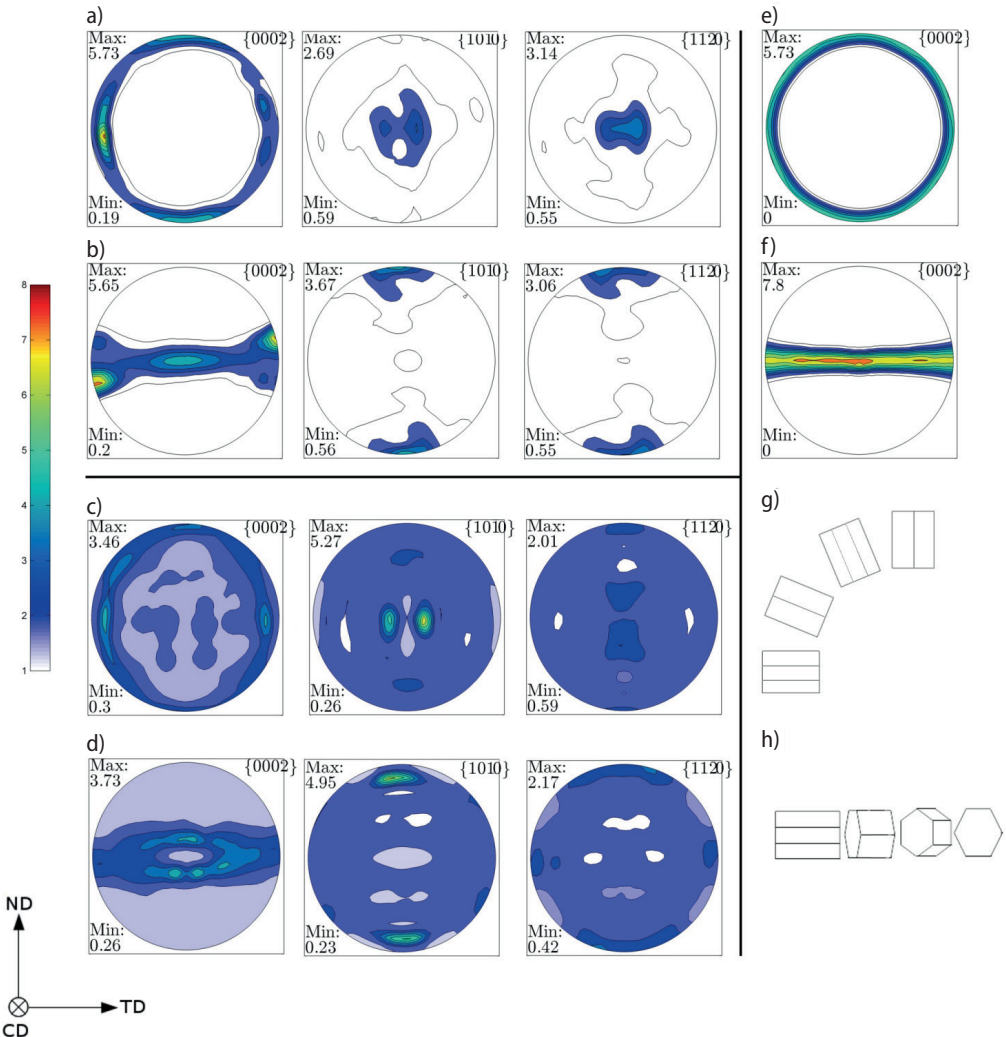

Fig. 1. Initial texture of samples A_{Mg} (a); B_{Mg} (b); A_{AZ61}(c); and B_{AZ61} (d); generated {0002} pole figures for simulations of sample Types A (e) and B (f); sketch showing alignment of HCP crystal cells in samples having texture Type A (g) and samples having texture Type B (h)

In the next step, the samples were deformed at room temperature at a strain rate of 10^{-3} s^{-1} up to 4% of the height reduction. The microstructure was investigated by using an optical microscope. The samples for the observations were first prepared on sandpaper followed by electro-polishing in a solution of orthophosforic acid in ethanol at a 3:5 ratio at 5V for 2 hours. After electro-polishing, the samples were etched with a picric acid reagent.

The texture evolution simulations were performed using the Taylor RC (relaxed constraints) model [16–19] for starting textures shown in Figures 1g and 1h. In the simulations, the slip systems and their critical resolved shear stress values (CRSS) shown in Table 1 were taken into account. In the present study, the twinning was treated as a regular slip system [1]. The texture evolution was calculated in 15 steps with a 0.005 effective strain step, giving a total of a 0.04 deformation. In the present study, strain rate tensor L and and relaxed constraints tensors K_1 and K_2 were as follows (see [17]):

$$L = \begin{bmatrix} 0.5 & 0 & 0 \\ 0 & 0.5 & 0 \\ 0 & 0 & -1 \end{bmatrix} \quad K_1 = \begin{bmatrix} 0 & 0 & 1 \\ 0 & 0 & 0 \\ 0 & 0 & 0 \end{bmatrix} \quad K_2 = \begin{bmatrix} 0 & 0 & 0 \\ 0 & 0 & 1 \\ 0 & 0 & 0 \end{bmatrix}$$

In Table 1, the CRSS for the slip systems taken to the simulations are presented [20–23].

Table 1. Parameters used during simulations [20–23]

Slip system	CRSS for Mg	CRSS for AZ61
$(0001)<11\bar{2}0>$	1	4
$\{10\bar{1}0\}<1\bar{2}10>$	10	7
$\{11\bar{2}2\}<\bar{1}\bar{1}23>$	20	7
$\{10\bar{1}2\}<11\bar{2}2>$	5	5

From the simulations, the Taylor factor (TF) and slip system activity were obtained.

3. Results and discussion

In Figure 2a, the work-hardening curves of deformed samples Types A and B for Mg and AZ61 are shown, and the corresponding microstructures are shown in Figures 2b, 2c, 2d, and 2e.

It can be seen that, in the case of the A_{Mg} and B_{Mg} samples, a significant difference in the work-hardening characteristics appears because of the initial texture. In the A_{Mg} samples (having a strong extrusion-type texture with the c-axis along a radial direction), the basal slip system is blocked during compression along the CD, and the main deformation mode is twinning. This is confirmed by Figure 2b, where a lot of twins can be

observed. The Type B_{Mg} samples deformed mainly by slip. In this case, the basal planes are arranged along a path between the TD and ND, allowing the basal slip system to be activated. Sample Types A_{AZ61} and B_{AZ61} do not show such differences despite a different initial texture. Both samples deform by slip with a comparison of twinning; however, it is believed that the twinning plays rather a secondary role.
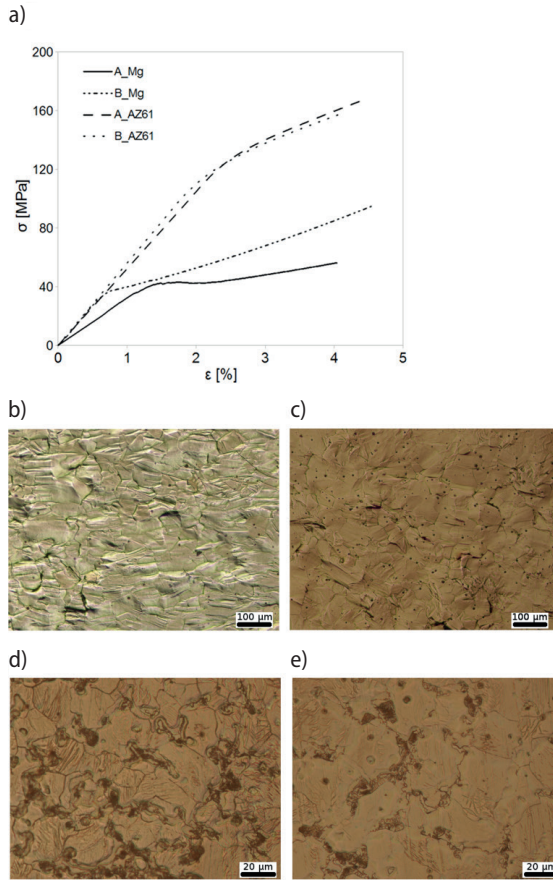

Fig. 2. Work-hardening characteristics of deformed samples A_{Mg}, B_{Mg}, A_{AZ61} and B_{AZ61} (a); micro-structure of samples after deformation up to 4% of samples A_{Mg} (b); B_{Mg} (c); A_{AZ61}(d) and B_{AZ61} (e)

In Figures 3a, 3b, 3c, 3d, and 3e, slip system activities are shown (obtained from the simulations according to the slip systems shown in Table 1). In Figures 3a and 3b, it can be seen that, in samples having a Type A texture (both Mg and AZ61), the basal slip system is almost inactive because of the reason mentioned above. In the case of the Type B texture, basal and non-basal slip systems are active, which can be observed in Figures 3c and 3d.
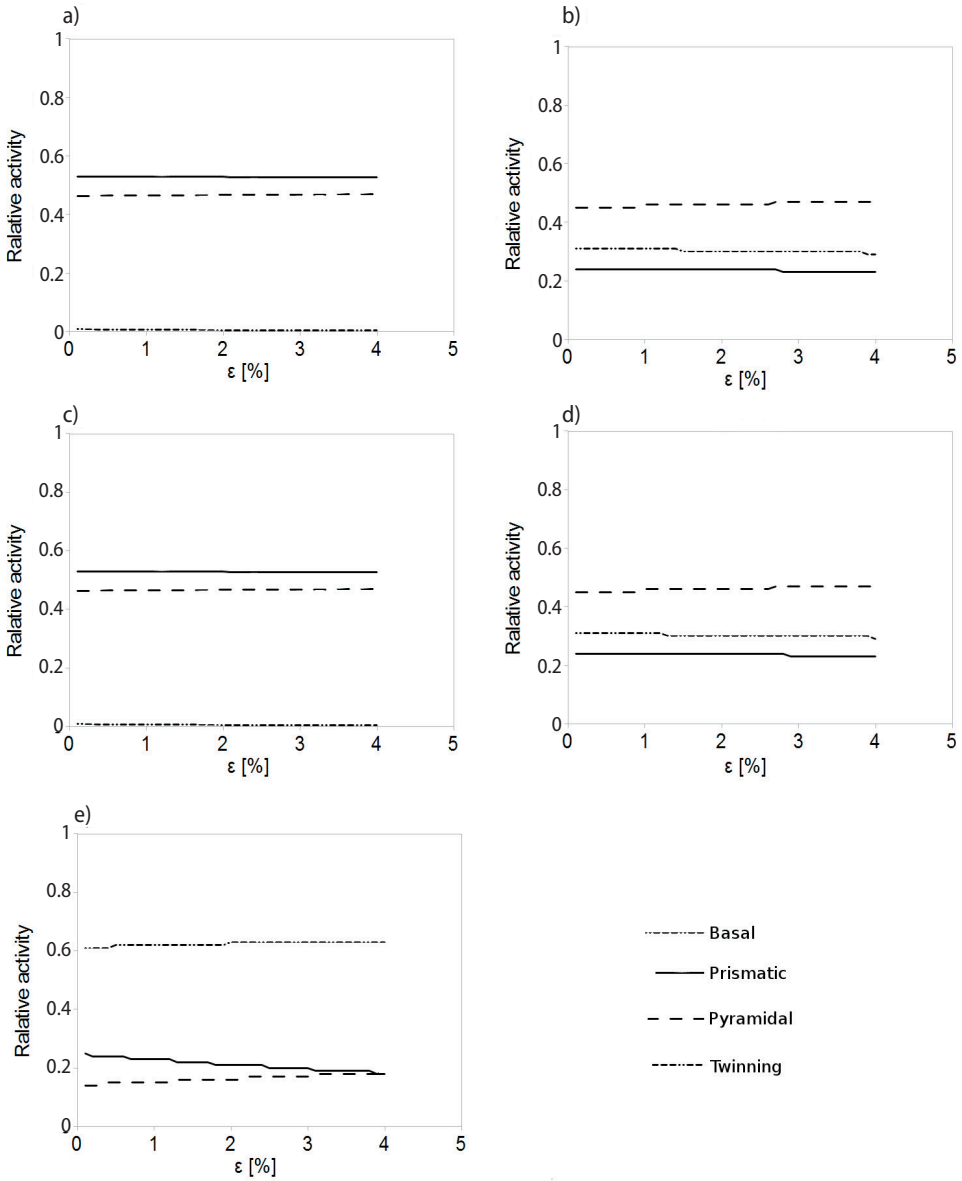
Fig. 3. Slip system activity obtained from simulations for sample Types A_{Mg}: a) without twinning; b) B_{Mg}; c) A_{AZ61}; d) B_{AZ61}; e) A_{Mg} with twinning

In Figure 4, the Taylor factor values for all of the investigated samples are presented. In Figure 4, it can be seen that, during the simulations of the texture evolution of A_{Mg} when no twinning was taken into account, the TF has the highest value (reaching 4.8).
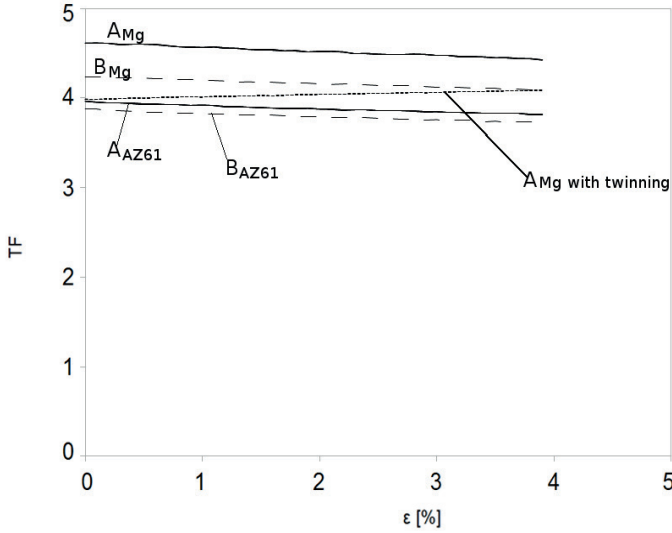
Fig. 4. Taylor factor (TF) values for samples A_{Mg}, B_{Mg}, A_{AZ61}, B_{AZ61}, and A_{Mg} while twinning was taken into account during texture evolution simulations. Slip systems are shown in Table 1

Shen et al. [19] investigated the TF evolution in pure magnesium and found it to be very high for hard slip modes (around 4.5); this is in agreement with the results obtained in the present study. It may be concluded that a TF value of about 5 is the maximum; thus, another mechanism other than slip must be considered in the case of Sample A_{Mg}. While twinning was introduced into the simulations of texture evolution in this study for sample Type A_{Mg}, the TF decreased to a value of 3.8. This means that, while the basal slip system is blocked in materials having strong textures (e.g., extrusion texture), twinning will activate to reduce the TF value. In the case of Samples A_{AZ61} and B_{AZ61} (which mainly deform by slip [basal and non-basal]), the TF has a lower value than in Sample A_{Mg} without twinning. The TF for A_{AZ61} is 3.9, and for B_{AZ61}, it is 3.8 because of the easy activation of the non-basal slip systems. It can be seen that the initial texture for AZ61 has rather no effect on the main deformation mode. The basal slip system is not active in the case of Samples A_{AZ61}, but the deformation in the non-basal slip systems (which have a very high values of CRSS [20–23]) results in TF values comparable to Sample A_{Mg}, where twinning was taken into account during the simulations (Fig. 3f). Thus, the twinning does not need to be activated during the deformation of the Type A and B AZ61 samples. The alloying elements reduce the CRSS for non-basal slip systems, making them easier to activate [20–23]; on the other hand, it increases the CRSS for basal slip systems, making it harder to activate. This explains why deformation by slip is the main deformation mode in both the A_{AZ61} and B_{AZ61} samples. However, different slip systems can be dominant rather than basal slip systems.

4. Summary

Based on the data in the present study several conclusions can be drawn.

1) Initial texture has an effect on the deformation mode in magnesium during compression.
2) Compression samples with an extrusion texture while the basal slip system is blocked involves twinning in pure magnesium.
3) Samples of A_{mg} exhibit the highest value of TF, in the case where twinning was not considered during simulations
4) Non-basal slip systems show a great deal of activity.
5) The value of the Taylor factor can be treated as a criterion for the activation of the deformation mode.
6) Sample Types A_{AZ61} and B_{AZ61} deform by slip in basal and non-basal slip systems.
7) The initial texture has a lesser effect on the samples of the AZ61 alloy than on the samples of pure magnesium.

References

[1] Gehrmann R., Frommert M.M., Gottstein G.: Texture effects on plastic deformation of magnesium. Materials Science and Engineering A, 395, 1–2 (2005), 338–349

[2] Wang W., Zhang W., Chen W., Cui G., Wang E.: Effect of initial texture on the bending behavior, microstructure and texture evolution of ZK60 magnesium alloy during the bending process. Journal of Alloys and Compounds, 737 (2018), 505–514

[3] Tadano Y.: Formability of magnesium sheet with rolling texture. International Journal of Mechanical Sciences, 108–109 (2016), 72–82

[4] Sułkowski B., Pałka P.: Deformation behavior of AZ61 magnesium alloy systematically rolled and annealed at 450°C. Kovové Materiály, 54, 3 (2016), 147–151

[5] Huang X., Suzuki K., Saito N.: Textures and stretch formability of Mg-6-Al-1Zn magnesium alloy sheets rolled at high temperatures up to 793K. Scripta Materialia, 60 (2009), 651–654

[6] Su J., Kabir A.S.H., Sanjari M., Yue S.: Correlation of static recrystallization and texture weakening of AZ31 magnesium alloy sheets subjected to high speed rolling. Materials Science & Engineering A, 674 (2016) 343–360

[7] Bian M.Z., Shin K.S.: {10 2} Twinning Behavior in Magnesium Single Crystal. Metals and Materials International, 19, 5 (2013), 999–1004

[8] Wang Y., Choo H.: Influence of texture on Hall–Petch relationships in an Mg alloy. Acta Materialia, 81 (2014), 83–97

[9] Martin É., Mishra R.K., Jonas J.J.: Effect of twinning on recrystallization textures in deformed magnesium alloy AZ31. Philosophical Magazine, 91, 27 (2011), 3613–3626

[10] Guan D., Rainforth W.M., Ma L., Wynne B., Gao J.: Twin recrystallization mechanism and exceptional contribution to texture evolution during annealing in a magnesium alloy. Acta Materialia, 126 (2017), 132–144

[11] Wang W., Zhang W., Chen W., Cui G., Wang E.: Effect of initial texture on the bending behavior, microstructure and texture evolution of ZK60 magnesium alloy during the bending process. Journal of Alloys and Compounds, 737 (2018), 505–514

[12] Huang X., Suzuki K., Chino Y.: Influences of initial texture on microstructure and stretch formability of Mg-3Al-1Zn alloy sheet obtained by a combination of high temperature and subsequent warm rolling. Scripta Materialia, 63 (2010), 395–398

[13] Zeng Z.R., Zhu Y.M., Xu S.W., Bian M.Z., Davies C.H.J., Birbilis N., Nie J.F.: Texture evolution during static recrystallization of cold-rolled magnesium alloys. Acta Materialia, 105 (2016), 479–494

[14] Wang Y.N., Huang J.C.: Texture analysis in hexagonal materials. Materials Chemistry and Physics, 81, 1 (2003), 11–26

[15] Graff S.: Micromechanical Modeling of the Deformation of HCP Metals. GKSS-Forschungszentrum Geesthacht GmbH, Geesthacht 2008

[16] Piehler H.R.: Crystal-Plasticity Fundamentals. In: ASM Handbook Volume 22A: Fundamentals of Modeling for Metals Processing, Furrer D.U., Semiatin S.L. (eds.), ASM International, Materials Park, Ohio, 2009, 232–238

[17] Van Houtte P.: A comprehensive mathematical formulation of an extended Taylor–Bishop–Hill model featuring relaxed constraints, the Renouard–Winterberg theory and a strain rate sensitivity model. Textures and Microstructures, 8–9 (1988), 313–350

[18] Van Houtte P., Li S., Seefeldt M., Delannay L.: Deformation texture prediction: from the Taylor model to the advanced Lamel model. International Journal of Plasticity, 21, 3 (2005), 589–624

[19] Shen J.H., Li Y.L., Wei Q.: Statistic derivation of Taylor factors for polycrystalline metals with application to pure magnesium. Materials Science & Engineering A, 582 (2013), 270–275

[20] Hutchinson W.B., Barnett M.R.: Effective values of critical resolved shear stress for slip in polycrystalline magnesium and other HCP metals. Scripta Materialia, 63, 7 (2010), 737–740

[21] Herrera-Solaz V., Hidalgo-Manrique P., Pérez-Prado M.T., Letzig D., Llorca J., Segurado J.: Effect of rare earth additions on the critical resolved shear stresses of magnesium alloys. Materials Letters, 128 (2014), 199–203

[22] Sánchez-Martín R., Pérez-Prado M.T., Segurado J., Bohlen J., Gutierrez-Urrutia I., Llorca J., Molina-Aldareguia J.M.: Measuring the critical resolved shear stresses in Mg alloys by instrumented nanoindentation. Acta Materialia, 71 (2014), 283–292

[23] Akhtar A., Teghtsoonian E.: Solid solution strengthening of magnesium single crystals – II: The effect of solute on the ease of prismatic slip. Acta Metallurgica, 17 (1969), 1351–1356